Biophysical Chemistry, 34 (1989) 9–18
Elsevier

BIOCHE 01367

Configurational and dynamic properties of different length superhelical DNAs measured by dynamic light scattering

Jörg Langowski and Ursula Giesen *

EMBL, Grenoble Outstation, 156X, F-38042 Grenoble Cedex, France

Received 2 February 1989
Revised manuscript received 12 April 1989
Accepted 12 April 1989

DNA; Superhelix; Dynamic light scattering; Rotational diffusion; Polymer internal motion

The solution conformation and internal motions of five superhelical DNAs between 2100 and 10200 base-pairs in length have been characterized by dynamic light scattering (DLS). Variations in the diffusion coefficients and rotational relaxation times with molecular weight are both indicative of an anisotropic extended structure of these DNAs; we therefore conclude that under our conditions the interwound superhelical structure prevails. The internal dynamics can be described by a superposition of rotational diffusion and internal relaxation. The latter process is characterized by the internal diffusion of persistence length size segments within the DNA chain and faster bending motions within these segments.

1. Introduction

Covalently closed circular DNA under torsional strain forms a 'superhelical' structure in solution [1]. The detailed structure of this superhelix is not yet well understood. Evidence exists for some superhelical DNAs that two conformations may occur [2,3]: an interwound form where two DNA double strands are wound around each other to form a more or less rod-like double spiral terminated by loops, or a toroidal form where the DNA double strand would be wound around the surface of an imaginary torus.

Our work contributes to resolving the problem of the general shape of an arbitrary superhelical DNA in solution, and elucidation of its dynamical properties, i.e., how the average structure is affected by chain flexibility and what fluctuations the shape may undergo. One approach to this question is to measure the configurational and dynamical properties of superhelical DNAs as a function of their length. From such studies, scaling laws may be derived which can provide us with insights into the average configuration of these large, geometrically constrained DNA chains. Specifically, hydrodynamic properties such as translational and rotational diffusion coefficients might differ between the toroidal and interwound configurations.

The second question addressed here is how to describe the internal motions in a superhelical DNA. Such a description will enable us to make more specific statements about the structure and its fluctuations. For example, the ionic strength dependence of internal motions in superhelical pUC8 DNA implies a very open but rather rigid structure at low salt, while at high salt the average shape seems to be unaltered but subject to much larger variations, suggesting strong fluctuations in local torsional strain [4].

Dynamic light scattering (DLS) has already yielded important information on DNA dynamics

Correspondence address: J. Langowski, EMBL, Grenoble Outstation, 156X, F-38042 Grenoble Cedex, France.
* Present address: ILL, 156X, F-38042 Grenoble Cedex, France.

(for a review, see ref. 5). In most previous work, an 'apparent diffusion coefficient' was measured by applying a single-exponential fit with relaxation time τ_r to the intensity scattering autocorrelation function and plotting $D_{app} = (2\boldsymbol{K}^2\tau_r)^{-1}$ as a function of the square of the scattering vector $\boldsymbol{K} = 4\pi n/\lambda \sin(\theta/2)$. Such a plot will extrapolate to the translational diffusion coefficient D_0 of the molecule as $\boldsymbol{K} \to 0$, and at very high $\boldsymbol{K}$ will approach a plateau value D_{plat} that is determined by the diffusion coefficient of the smallest independently moving subunit within the polymer coil envelope (Rouse-Zimm subunit [6,7]). D_0, D_{plat} and the form of the transition in the intermediate-$\boldsymbol{K}$ region have been used to characterize the structure and dynamics of various types of DNA in solution [8]. Empirical correlations of D_{plat} with torsional rigidity, the presence of titratable joints, buffer composition and DNA conformation could be established.

The direct connection of D_{app} as a function of $\boldsymbol{K}^2$ with fundamental physical parameters of the DNA is still unclear. Specifically, the intermediate-$\boldsymbol{K}$ region shows a multi-exponential correlation function and the forced single-exponential fit is therefore only an approximation. It has been shown by Pecora's group [22,25] and in our work [9] that the correlation function in this region can be approximated by a bimodal exponential distribution, and in ref. 25 these modes have been associated with relaxation modes obtained from a free-draining Rouse-Zimm model. In fact, for small superhelical DNAs such as pUC8 (2717 base-pairs) the bimodal distribution is very well approximated by two superimposed exponential decays [9]. Their decay rates are proportional to $\boldsymbol{K}^2$ and may therefore be described by diffusion coefficients; the slow mode corresponds to the translational diffusion coefficient D_0 and the fast mode to an 'internal diffusion coefficient' D_i which is related to the persistence length of the DNA.

In the low-$\boldsymbol{K}$ region, where the theory demonstrates that the correlation function of an anisotropic, rigid particle simplifies to a superposition of two discrete exponential modes, we observed a rapidly relaxing component of small amplitude that corresponds to the end-over-end rotational tumbling of the interwound DNA structure. We attempt in the present paper to generalize our description to DNAs of different molecular weight, extracting the rotational relaxation time and the internal diffusion coefficient as convenient parameters.

2. Materials and methods

2.1. Preparation of plasmid DNA

The plasmids used were pLN1 (2100 bp; courtesy of J.H. van de Sande, Calgary), pBR322 (4363 bp), pACL29 (5400 bp; courtesy of G. Cesareni, Heidelberg) and pDR1996 (10200 bp; courtesy of I. Bayer, Hannover).

Plasmids were grown in *E. coli* strain HB 101 and prepared by lysozyme/SDS lysis, poly(ethylene glycol) (PEG) precipitation and CsCl/ethidium density gradient centrifugation as described previously [10]. The purity of the DNA was checked by agarose gel electrophoresis; none of the samples investigated was less than 95% superhelical before and 80% superhelical after the experiment. All experiments were in 0.1 M NaCl, 5 mM sodium phosphate, 1 mM EDTA (pH 7.0).

2.2. Dynamic light scattering

Scattered light intensity autocorrelation functions (ACFs) were collected on either of two systems: (1) a goniometer of our own construction with a Coherent Innova 90-6 argon ion laser running at a power of 400–600 mW at 488 nm, EMI 9863 QB-100 photomultiplier and data analysis on a Brookhaven Instruments BI-2030 4 by N-bit autocorrelator with 136 real time channels and multiple sample time option or (2) an AMTEC goniometer with a Spectra-Physics 165 argon ion laser running at 400–600 mW at 488 nm, the same photomultiplier and a Malvern K7023 1 by N-bit autocorrelator with 88 + 4 delay channels.

In both systems, the control programs contained 'software dust filters' [4] which ensured that parts of the photon pulse stream contaminated by dust 'tyndalls' were not accumulated into the ACF. This was achieved by collecting the data in short periods of 2–5 s, retaining only those

curves which were below a preset intensity threshold and whose calculated baselines (from the total photon count) differed from those measured (from the last delay channels) by less than 0.5%. The baseline difference on the accumulated data is then typically less than 0.05%. The procedure speeds up the data collection for a given signal-to-noise ratio by a factor of approx. 2–3.

2.3. Data evaluation

We assume that the first-order autocorrelation function $G^{(1)}(\tau)$ of a flexible DNA chain can be expressed as a sum of decaying exponentials. This assumption is correct in the limit of small scattering vectors ($K^2 < 2 \times 10^{14}[\mathrm{m}^{-2}]$), and is a good empirical approximation [4,9] for larger K^2. The second-order autocorrelation function $G^{(2)}(\tau)$ then becomes:

$$G^{(2)}(\tau) = 1 + \left(\sum_{i=1}^{n_{\max}} e^{-\tau/\tau_i} \right)^2 \quad (1)$$

To account for small baseline deviations, we fit the function

$$G^{(2)}(\tau) = A + \left(\sum_{i=1}^{n_{\max}} e^{-\tau/\tau_i} \right)^2 \quad (2)$$

to the measured ACF using a nonlinear least-squares fitting program based on subroutine VA05A from the Harwell subroutine library (C. Urbanke and J. Greipel, unpublished data); alternatively, we used the fitting program DISCRETE [11] to fit a sum of single exponentials to $G^{(1)}(\tau)$, which was approximated by

$$G^{(1)}(\tau) \approx \mathrm{sign}\left(G^{(2)}(\tau) - 1\right) \cdot \sqrt{|G^{(2)}(\tau) - 1|} \quad (3)$$

No significant deviations were observed between fits using eq. 2 or the DISCRETE program. The results reported here were obtained using eq. 2.

3. Results

The results of forced single-exponential fits to the scattered intensity ACF are displayed in fig. 1. Although the residuals of the fit obtained in this manner clearly show correlations, we show the D_{app} data for comparison with results from the literature obtained in a similar fashion. We note the general shape of the curves, which for $K^2 \to 0$ extrapolate to the translational diffusion coefficient of the DNA, and increase monotonically for larger K. The curves do not level off to a plateau even at the greatest value of K studied here, although they will eventually do so in ultraviolet light scattering [12].

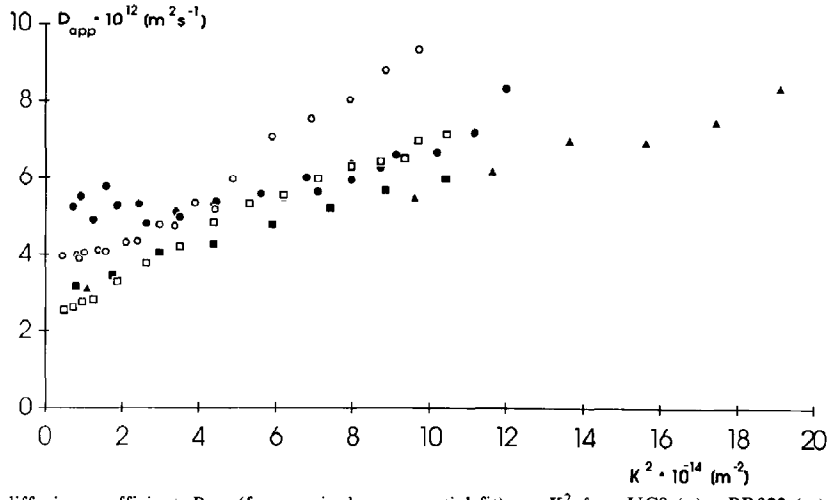

Fig. 1. Apparent diffusion coefficient D_{app} (from a single-exponential fit) vs. K^2 for pUC8 (●), pBR322 (○), pACL29 (■, ▲), and pDR1996 (□).

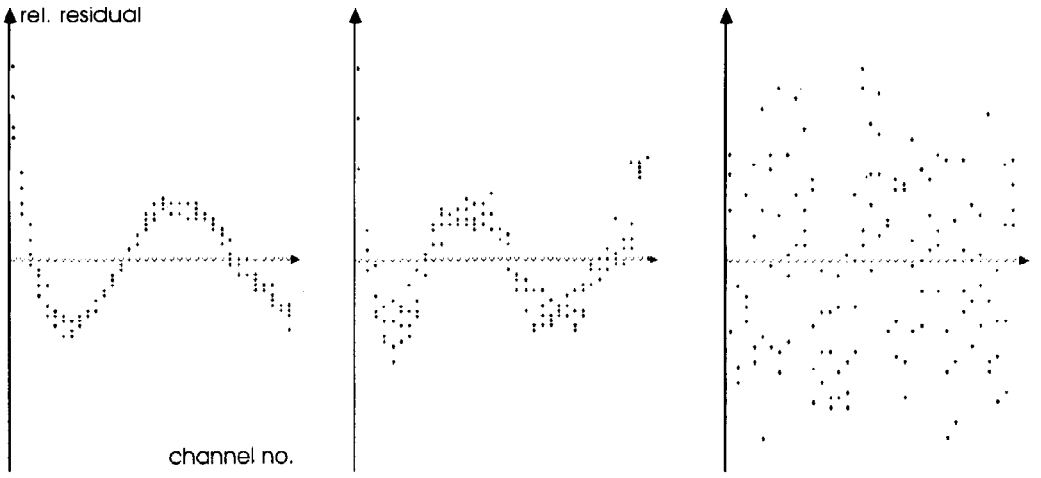

Fig. 2. Residuals of one-, or two- and three-exponential nonlinear least-squares fit (from left to right) to the scattered light intensity autocorrelation function of pBR322 measured at $K^2 = 9.4 \times 10^{14}$ m^{-2}. Abscissa indicates successive correlator channels; ordinate scale decreases from left to right. The standard deviation decreased by a factor of 20 on going from a one- to a three-exponential fit.

Fig. 2 shows a comparison of the residuals of a one-, two- and three-component fit of eq. 2 of a typical data set measured on pBR322. It is evident that a multiexponential fit with two to three relaxation components is needed to describe the data in an appropriate way. The predictions using DISCRETE yield the same number of components as predicted from visual inspection of the residuals.

For the larger plasmids, pBR322, pACL29 and pDR1996, we found that above $K^2 = 2\text{–}3 \times 10^{14}$ m^{-2} the two-component fit was unsatisfactory and a third component had to be included. The autocorrelation function of pUC8 (2717 bp) could be well described by two exponential components, as shown before [4,9]. The pLN1 sample (2100 bp) contained a third, slow component, which was due to dust or aggregate contamination in this sample; in this case only the two faster components were taken to correspond to the translational and internal diffusion contributions.

The slow component extrapolated to $K^2 \to 0$ yields the translational diffusion coefficient, D_t, of the molecule in a more accurate way than direct extrapolation of D_{app} to $K^2 \to 0$, since the fast contributions have been taken into account separately in the fit. D_t varies with the molecular weight (M) of DNA as $D_t \propto M^{-0.6}$ (fig. 3). A stiff rod would have a molecular weight dependence of $D_t \propto M^{-0.8}$, while for a Gaussian coil $D_t \propto M^{-0.5+\epsilon}$, the excluded volume exponent ϵ for linear DNA being $\epsilon = 0.05$ at 0.1 M ionic strength [13]. The value we obtain therefore lies slightly above that of the Gaussian coil.

We then approached the question as to the expected molecular weight dependence of the diffusion coefficients of the toroidal and interwound superhelices on DNA contour length. For a rigid interwound form, theoretical work by several

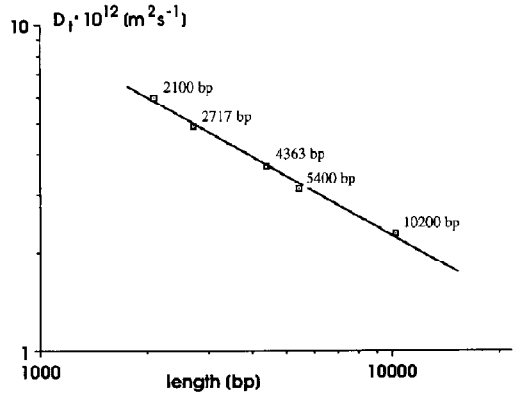

Fig. 3. Translational diffusion coefficient D_t of superhelical plasmid DNA as a function of length. The regression line corresponds to a power law of $D_t \propto M^{-0.6 \pm 0.1}$.

groups [14,15] has led to the conclusion that the radius of the interwound form should be independent of DNA length; under this assumption and for a rigid structure, a dependence close to that of a rigid rod ($D_t \propto M^{-0.8}$) should be obtained, with the exponent decreased due to flexibility.

For a rigid toroid, on the other hand, a $D_t \propto M^{-0.8}$ dependence would only be valid under the assumption that the coil radius stayed constant while the outer radius increased in proportion to the DNA filament length. This is unlikely for a structure at elastic equilibrium; rather, it is probable that a toroidal structure would show a dependence similar to that of the Gaussian coil ($D_t \propto M^{-0.5}$). The value that we find lies between the extremes of a rigid rod and a Gaussian coil; we conclude that the superhelix structure is more extended than a perfect toroidal shape, but not completely rigid.

Further evidence for a rotationally anisotropic structure is provided by an analysis of the faster components of the autocorrelation function. As $\boldsymbol{K}^2 \to 0$, the dynamic structure factor of an anisotropic particle with characteristic dimensions of the order of $|\boldsymbol{K}|^{-1}$ or larger contains a $\boldsymbol{K}$-independent fast relaxation time τ_r, which is related to the end-over-end rotational diffusion coefficient Θ_r of the particle by $\tau_r = 6\Theta_r$ as shown by Pecora [16].

Spherical particles will show no such component; the fact that a plot of the internal relaxation rate vs. $\boldsymbol{K}^2$ has a nonzero intercept (fig. 4) is therefore an indication that the particle is anisotropic. It has been shown previously [4] that the fast rapid relaxation rate does approach zero for $\boldsymbol{K}^2 \to 0$ when a 2717 base-pair DNA is linearized, this molecule then assuming an isotropic Gaussian-coil shape.

From the intercepts in fig. 4, rotational diffusion coefficients can be calculated for all of the

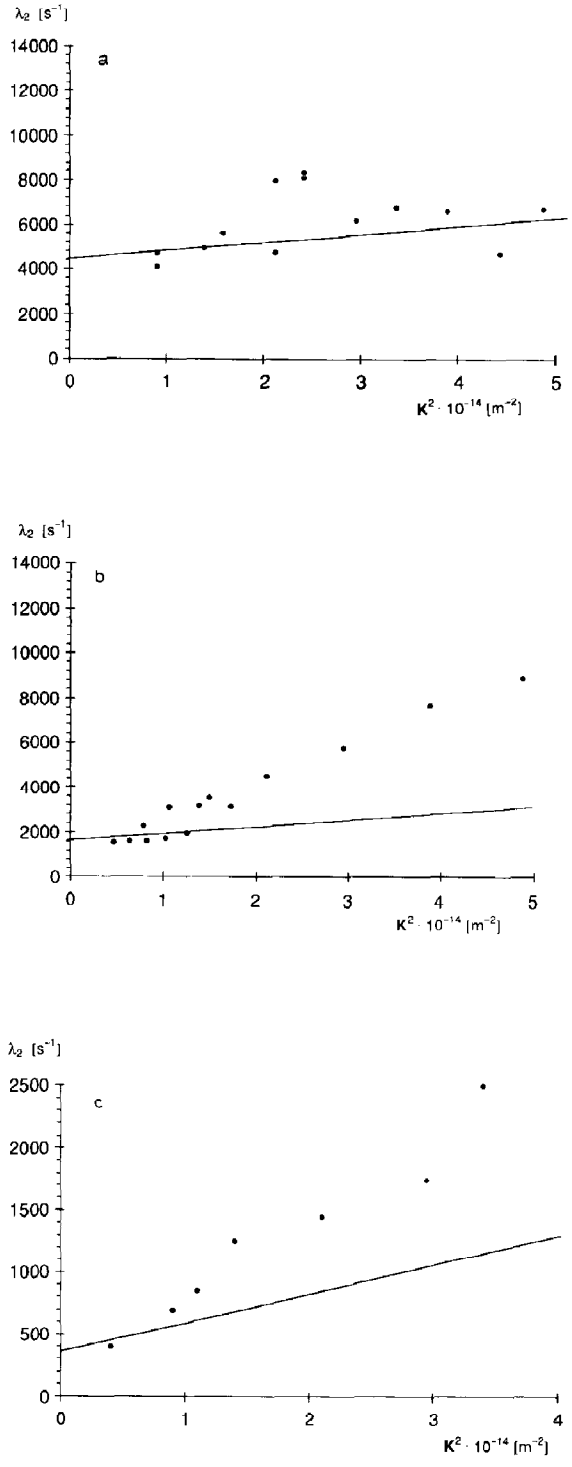

Fig. 4. First internal relaxation rate from a multiexponential fit vs. $\boldsymbol{K}^2$. (a) pBR322, (b) pACL29, (c) pDR1996. Extrapolation to $\boldsymbol{K}^2 = 0$ with slope $= D_t$ gives the end-over-end rotational tumbling rate of the DNA. The corresponding curve for pUC8 has been published in ref. 4.

plasmid DNAs studied except for pLN1, where the fast relaxation data become too unreliable at low K due to the contamination (fig. 5). Even for the largest plasmid, pDR1996 (10200 base-pairs), the plot still shows a nonzero intercept, although the extrapolation becomes less reliable. The extrapolation was performed by fitting a line with slope given by D_0 through the points at $K^2 < 2 \times 10^{14}$ m^{-2}.

The rotational diffusion coefficient has a dependence according to $M^{-2.7 \pm 0.3}$ (fig. 5), in agreement with a flexible rod-like structure: a stiff rod would vary as a function of M^{-3}, while a rigid toroidal structure with toroid main radius and cross-sectional radius increasing in equal proportions should depend approximately on M^{-2}. Flexibility would decrease both exponents.

3.1. Internal motions at high scattering vectors

At high scattering angles, the relaxation rates can be characterized by unique diffusion coefficients: the lowest, D_t, corresponds to translational diffusion, the greater terms, $D_i^{(1)}$ and $D_i^{(2)}$, to internal motions. The fast components for the plasmids studied are displayed in fig. 6 as averages over the range $K^2 = 4$–10×10^{14} m^{-2}, where the D_i values no longer showed any significant variation.

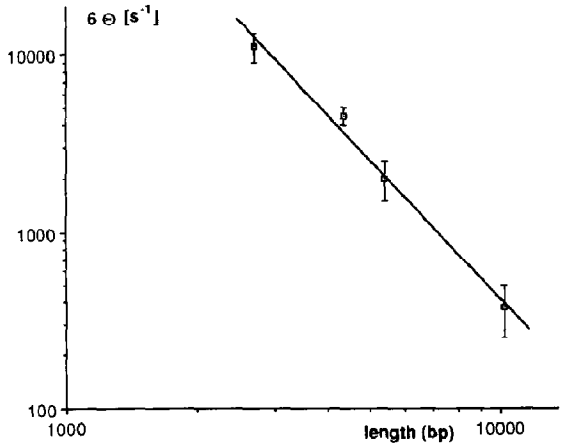

Fig. 5. End-over-end rotational diffusion constant Θ_r of superhelical plasmid DNA as a function of length. The regression line corresponds to a power law of $D_t \propto M^{-2.7 \pm 0.3}$.

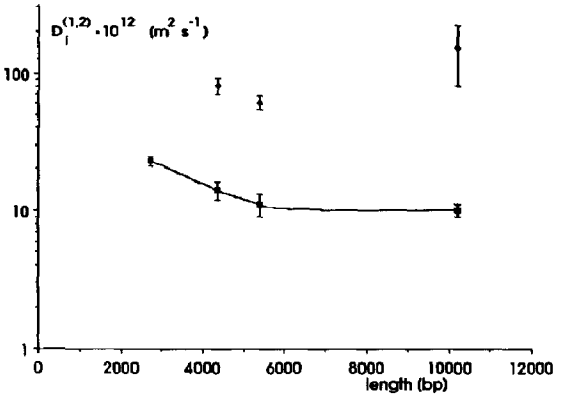

Fig. 6. Length dependence of the 'internal diffusion coefficients' $D_i^{(1)}$ and $D_i^{(2)}$ obtained from the fast relaxation time(s) in the light scattering autocorrelation functions for superhelical DNA.

We have shown previously [4,9] that the internal motions of pUC8 can be well described by one internal diffusion coefficient $D_i = 20$–25×10^{-12} m^2 s^{-1} at high K; at low K ($< 2 \times 10^{14}$ m^{-2}) D_i apparently increases, which is due to the rotational contribution mentioned above.

This finding can now be generalized: the main contribution to the internal motions of all plasmids studied here is due to internal segment diffusion with diffusion coefficient $D_i^{(1)} = 10$–$25 \cdot 10^{-12}$ m^2 s^{-1}. For the larger plasmid, a small amplitude of a fast component with $D_i^{(2)} = 50$–100×10^{-12} m^2 s^{-1} must be taken into account (fig. 6). Since an exponential distribution analysis shows only two peaks, these two discrete internal components reflect a distribution of the relaxation times of internal motion.

4. Discussion

For all superhelical plasmid DNAs investigated here, the apparent diffusion coefficient D_{app} increases with scattering vector K, as expected for a flexible polymer [5]. This increase is due to internal motions of the polymer chain, and to rotational motions of the anisotropic molecule as a whole. Extrapolation of D_{app} to $K^2 = 0$ yields the translational diffusion coefficient D_t of the DNA; this quantity, however, can be determined with

much greater accuracy by extrapolating the slowest component D_1 of a two- or three-exponential fit to the autocorrelation function.

The multiexponential fitting procedure gives reliable values for the diffusion coefficients of even the longest superhelical DNAs studied here, even though the curve D_{app} vs. K^2 increases rather steeply at low K (fig. 1). We find a molecular weight dependence of the translational diffusion coefficient of superhelical DNA of $D_t \propto M^{-0.6}$. From the intercept of a plot of the fast relaxation rate. vs. K^2, we obtain the rotational diffusion coefficient Θ_r of the particle, which varies with respect to $M^{-2.7 \pm 0.3}$ (fig. 5). Since the quantity is, to a first approximation, inversely proportional to the third power of the longest dimension of the particle [18], the maximum extension of the superhelices studied here would be dependent upon $M^{-0.9 \pm 0.1}$.

The length dependence alone proves neither a toroidal nor interwound structure, since the longest linear dimension of both structures would be proportional to the molecular weight if the cross-section were independent of the length of the DNA. In a toroid the elastic energy of bending is distributed between the local bending of the DNA double helix around the toroid cross-section and the bending of the DNA solenoid into the toroid shape [19], while in a rod-like interwound structure this force is only due to the bending of the DNA double helix around the cross-section of the rod. Therefore, increasing the contour length of an interwound superhelical DNA at constant superhelical density will have no influence on the local bending forces, while a toroidal structure will have higher bending energy for short contour length at constant superhelical density.

Since the forces that determine the local structure of an interwound superhelix are only dependent on supercoil density, electrostatic interactions between strands, and local elasticity, the cross-sectional radius of an interwound structure is independent of contour length. The end-to-end distance of the superhelix is then proportional to the contour length, with deviations due to flexibility, and its hydrodynamic parameters scale like those of a semiflexible rod.

From the rotational tumbling times, average end-to-end distances l_{rot} of the interwound superhelix – assuming rod-like structures – may be calculated [24]. Table 1 summarizes the results of these calculations together with the contour lengths $l_{f.e.}$ of a maximally extended interwound structure. We assumed a 40 : 1 axial ratio for the cylinder in the rotational diffusion calculation (for long cylinders, the result depends only very slightly on this ratio).

The ratio between the end-to-end distance from the rotational diffusion and the maximum extension is the same for all four plasmids; 0.41 ± 0.03. This 'shrinkage' is due to two contributions: (a) the wrapping of the DNA double helix axis around the imaginary superhelix surface, and (b) flexibility of the superhelix itself. The former can be estimated from the superhelix pitch angle, which we assume to be 45°, in agreement with theoretical considerations by Camerini-Otero and Felsenfeld [14]. This pitch angle leads to an end-to-end distance of the superhelix of $(1/\sqrt{2})$-times its maximum value. The remaining shrinkage factor of 0.58 must then be due to flexing of the superhelix itself.

With the relationship between the mean-squared end-to-end distance of a flexible polymer, $\langle h^2 \rangle$,

Table 1

Average dimensions of four superhelical DNAs of different length in solution

DNA	Length (bp)	$l_{f.e.}$ (nm)	$l_{45°}$ (nm)	l_{rot} (nm)	l_{rot}/l_{fe}	a_{app} (nm)
pUC8	2717	462	327	204	0.44	127
pBR322	4363	742	525	278	0.38	147
pACL29	5400	918	649	390	0.43	234
pDR1996	10200	1734	1226	700	0.40	400

its persistence length a and contour length L, $\langle h^2 \rangle = La$, we can calculate a first-guess approximation of the persistence length of the interwound superhelix. The contour length of the superhelix is taken as the end-to-end distance of a straight interwound rod-like structure with 45° pitch, $l_{45°}$, and the solution end-to-end distance, l_{rot}, is taken from the rotational diffusion data. Table 1 shows apparent persistence lengths a_{app} estimated from $a_{app} = (l_{rot})^2/l_{45°}$. This 'persistence length' increases with the length of the DNA, which is not surprising due to the $M^{-2.7}$ dependence of the end-to-end distance. Since superhelical DNAs, even of length 10000 base-pairs, do not show Gaussian coil behavior, the actual persistence length of the symmetry axis of a superhelix might be equal to or greater than 400 nm.

The internal diffusion coefficients that correspond to the fast components of the light scattering autocorrelation function are only slightly dependent on molecular weight. In a previous paper [4], we proposed that the internal diffusion coefficient D_i found on the plasmid pUC8 characterizes the mutual internal motion of persistence length ($\approx$ 200 bp) DNA segments within one DNA molecule.

For the larger plasmids studied here, two internal diffusion coefficients $D_i^{(1)}$ and $D_i^{(2)}$ are needed to describe the internal motions. $D_i^{(1)}$, which constitutes the major part of the internal motions, is of the same order of magnitude as our previously found D_i, while $D_i^{(2)}$ would correspond to a small amplitude of motions of even smaller segments.

Preliminary inelastic neutron scattering data [20] indicate that the fastest independent motion within both linear and superhelical DNAs (the plateau value of the D_{app} vs. K^2 curve) corresponds to a diffusion coefficient of approx. 15×10^{-12} m^2 s^{-1} for a 5400 base-pair DNA, which agrees well with the $D_i^{(1)}$ obtained here. We may therefore identify this quantity with the diffusion coefficient of the Rouse-Zimm subunit of the DNA chain.

As in our previous experiments, we can compare this internal diffusion coefficient with the diffusion coefficient expected for a persistence length-size DNA piece. Assuming the persistence length to be 50 nm, a rigid rod of that length and 2.5 nm diameter would have a diffusion coefficient [21] of 30×10^{-12} m^2 s^{-1}. We may thus assign $D_i^{(1)}$ to the motion of DNA segments of an average two to three persistence lengths within the polymer coil. The decrease of $D_i^{(1)}$ with increasing plasmid length shows that only for the larger DNAs do we actually observe completely independent segmental motion, with the average segment length being three persistence lengths; for the smaller DNAs, the observed segment length is smaller.

$D_i^{(2)}$, only seen in the larger plasmids where the total amplitude of internal motion is high enough, corresponds to even faster motions. However, such motions cannot correspond to smaller independent subunits, since otherwise the plateau diffusion coefficient would be greater than that observed in the neutron scattering data. Rather, this motional component probably corresponds to bending/torsion on a smaller length scale than the persistence length.

The relative amplitude of the fast relaxation component a_2 increases with scattering angle, as expected. Without assuming any particular functional behavior of a_2 vs K^2, we simply approximate this increase by a straight line. The average slope m_2 of such plots for the four larger plasmids (in units of 10^{-14} m^2) is 0.12 ± 0.01 (pUC8), 0.3 ± 0.02 (pBR322), 0.2 ± 0.01 (pACL29), and 1.0 ± 0.02 (pDR1996). The result seems to indicate that the internal motions of the four plasmids fall within two qualitatively different groups. The contribution of the fast component should depend, to a first approximation, on the square of the radius of gyration of the molecule, as has been pointed out previously [26]. In our case, we can assume that the radius of gyration is approximately proportional to the hydrodynamic radius R_h, obtained from the translational diffusion coefficient D_t, $R_h = k_b T/6\pi\eta D_t$. Therefore, the quotient of the slope of the a_2 vs. K^2 plot and R_h^2 should be approximately the same for all molecules with comparable behavior of the internal motion. This value, m_2/R_h^2, for the four plasmids is 0.65 (pUC8), 0.94 (pBR322), 0.43 (pACL29), and 1.05 (pDR1996). We thus see that pBR322 and pDR1996 have m_2/R_h^2 values close to 1.0,

whereas those of pUC8 and pACL29 are around 0.5. This correlates with the fact that the D_{app} vs. K^2 curves for pBR322 and pDR1996 show a steeper slope in the intermediate-K region than pUC8 and pACL29. This phenomenon merits further study, and the parameter m_2/R_h^2 seems to be a convenient quantity to characterize the internal motion of semiflexible polymers.

Recently, Lewis et al. [22] and Sorlie and Pecora [25] published DLS studies on DNA internal motions. In ref. 22, the length dependence of the DLS from variable-length supercoiled plasmid DNAs was studied at two scattering angles, 20–30 and 90°. At both of these angles, their results are similar to ours. Their data analysis is based on the CONTIN program [23], which gives a bimodal distribution for the 90° data. The mean values of the peaks of the bimodal distribution are then interpreted as two discrete relaxation times, corresponding to segment rotation and being independent of the total length of the plasmid DNA.

The bimodality of the exponential distribution at intermediate scattering angles is similar to our findings [9]; however, in ref. 22 the angular dependence of the two components has not been determined and one cannot say with certainty whether they are 'diffusive', i.e., with relaxation rate proportional to the square of the scattering vector, or behave differently. Our data, measured over a range of scattering vectors, clearly show that in the high-K regime the internal motions of superhelical DNAs are diffusive while at low K they are 'rotational', i.e., K-independent.

The power – and the disadvantage – of an inverse Laplace transform program like CONTIN is that no assumption is made about the actual form of the distribution, except that it is smooth and contains no negative components. Therefore, CONTIN will produce a rather smooth uni- or bimodal distribution even on data that contain discrete exponentials. This problem has been overcome in the more recent paper by Sorlie and Pecora [25], where theoretical data from a free-draining Rouse-Zimm model with simulated experimental noise were subjected to the same CONTIN analysis as the experimental data. This allows better interpretation of the data in the intermediate-K range, however, at very low K still only one exponential component is observed.

When the additional knowledge that the autocorrelation function must be composed of a squared sum of discrete exponentials in the limit of low K is applied to the data analysis, it can be seen clearly that two components are required for a good fit. A CONTIN analysis in this region will suppress the small amplitude of the rotational component, at least for data of the precision obtained here.

We have not attempted to give more than a qualitative explanation of the internal motion components of the DNAs studied here, the question of a theory for semiflexible chains being still a very open one. Nevertheless, the description of DNA internal motions in terms of a multiexponential decomposition should be an important test for existing and new theories and makes parameters available that serve to describe qualitatively the dynamics of DNA beyond the notion of a homogeneous elastic filament. For low scattering vectors, where reasonable theories are available, the multiexponential data analysis allows us to establish that the superhelical DNAs form an anisotropic structure in solution and to estimate its size and shape. Model calculations are underway which will correlate the parameters measured here with plausible models for superhelical DNA.

Acknowledgements

We thank Professor G. Maaß and Dr. C. Urbanke for supporting and discussing this work, which was in part conducted at the Institut für Biophysikalische Chemie, Medizinische Hochschule, Hannover, F.R.G. Thanks are also due to C. Lehmann for help with plasmid preparations and E. Schuppe for expert mechanical work. Finally, we are grateful to one of the referees for constructive comments, especially the suggestion of comparing the progression of relative amplitudes of the rapidly relaxing component for the different DNAs. This project was supported by grants La 500/2 and La 500/3 of the Deutsche Forschungsgemeinschaft to J. L.

References

1 W.R. Bauer, Annu. Rev. Biophys. Bioeng. 7 (1978) 287.
2 G.W. Brady, D. Foos and C.J. Benham, Biopolymers 23 (1984) 2963.
3 A. Campbell, Biochem. J. 171 (1978) 281.
4 J. Langowski, Biophys. Chem. 27 (1987) 263.
5 J.M. Schurr and K.S. Schmitz, Annu. Rev. Phys. Chem. 37 (1986) 271.
6 P.E. Rouse, J. Chem. Phys. 21 (1953) 1272.
7 B.H. Zimm, J. Chem. Phys. 24 (1956) 269.
8 S.C. Lin and J.M. Schurr, Biopolymers 17 (1978) 425.
9 J. Langowski, U. Giesen and C. Lehmann, Biophys. Chem. 25 (1986) 191.
10 J. Langowski, A.S. Benight, B.S. Fujimoto and J.M. Schurr, Biochemistry 24 (1985) 4022.
11 S. Provencher, Biophys. J. 16 (1976) 27.
12 J.M. Schurr, Chem. Phys. 30 (1978) 243.
13 D. Stigter, Macromolecules 18 (1985) 1619.
14 R.D. Camerini-Otero and G. Felsenfeld, Proc. Natl. Acad. Sci. U.S.A. 75 (1978) 1708.
15 H. Tsuru and M. Wadati, Biopolymers 25 (1986) 2083.
16 B. Berne and R. Pecora, Dynamic light scattering (Wiley, New York, 1976).
17 T. Maeda and S. Fujime, Macromolecules 17 (1984) 2381.
18 F. Perrin, J. Chem. Phys. 10 (1942) 415.
19 C.J. Benham, Biopolymers 22 (1983) 2477.
20 J. Langowski, U. Giesen and B. Farago, in: Laser scattering spectroscopy of biological objects, eds. J. Štěpánek, P. Anzenbacher and B. Sedláček (Elsevier, Amsterdam, 1989) in the press.
21 M.M. Tirado and J. Garcia de la Torre, J. Chem. Phys. 71 (1979) 2581.
22 R. Lewis, J.H. Huang, and R. Pecora, Macromolecules 18 (1985) 944.
23 S.W. Provencher, CONTIN V2 user's manual, EMBL technical report DA07, Heidelberg (1984).
24 M.M. Tirado and J. Garcia de la Torre, J. Chem. Phys. 73 (1980) 1990.
25 S.S. Sorlie and R. Pecora, Macromolecules 21 (1988) 1437.
26 M. Caloin, B. Wilhelm and M. Daune, Biopolymers 16 (1977) 2091.